A&A 419, L43–L47 (2004)
DOI: 10.1051/0004-6361:20040139
© ESO 2004

Astronomy & Astrophysics

Stellar dynamics of blue compact galaxies⋆

I. Decoupled star–gas kinematics in ESO 400-G43

G. Östlin[1], R. J. Cumming[1], P. Amram[4], N. Bergvall[2], D. Kunth[5], I. Márquez[3], J. Masegosa[3], and E. Zackrisson[2]

[1] Stockholm Observatory, AlbaNova University Center, 10691 Stockholm, Sweden
[2] Uppsala Astronomical Observatory, Box 515, 75120 Uppsala, Sweden
[3] Instituto Astrofisica de Andalucia (CSIC), Camino Bajo de Huetor 24, 18008 Granada, Spain
[4] Observatoire Astronomique Marseille-Provence & Laboratoire d'Astrophysique de Marseille, 2 place Le Verrier, 13248 Marseille Cedex 4, France
[5] Institute d'Astrophysique de Paris, 98bis boulevard Arago, 75014 Paris, France

Received 12 March 2004 / Accepted 10 April 2004

Abstract. In this *letter* we present the first results from a program aimed at measuring the stellar kinematics of blue compact galaxies by observing the near-infrared Calcium triplet. We show the first results for ESO 400-G43 based on deep VLT/FORS2 spectroscopy. The instabilities found in the central gaseous velocity field are not seen in the solid body stellar rotation curve, indicating that stars and gas are kinematically decoupled in this galaxy. Even if this galaxy has a perturbed gaseous velocity field, the stellar velocity dispersion on average agrees well with that derived from the nebular lines.

Key words. galaxies: compact – galaxies: kinematics and dynamics – galaxies: individual: ESO400-G43 – galaxies: starburst

1. Introduction

There has been strong interest in Blue Compact Galaxies (BCGs) ever since the pioneering study of Searle & Sargent (1972). The hypothesis that BCGs represent genuinely young galaxies, presently forming their first generation of stars, has now been disproved for all but a few extreme cases (see, e.g., Kunth & Östlin 1983 for a review). However, the evolutionary history of BCGs, their connection to other kinds of galaxies, and the mechanism that triggers the active star formation are still elusive.

Most studies of the nature of BCGs have been based on surface photometry (e.g. Papaderos et al. 1996) or spectroscopic analysis of nebular abundances (e.g. Izotov & Thuan 1999), and relatively little is known about their dynamics, though HI velocity fields have been obtained for some galaxies (e.g. van Zee et al. 1998). The stellar component has been much less analysed than the gaseous one because the spectra are dominated by hot stars and ionised gas emission, diluting stellar absorption features in the optical domain and making kinematical and chemical analysis difficult.

In Östlin et al. (1999, 2001) we investigated the velocity fields of the ionised gas in BCGs, using the CIGALE Fabry-Perot interferometer (Amram et al. 1991) and targeting the Hα line. These results show that many luminous BCGs (LBCGs) have peculiar Hα velocity fields and irregular morphology, suggesting that their starbursts have been triggered by dwarf galaxy mergers. Many LBCGs also rotate too slowly to support the stellar mass inferred from deep optical and near-IR photometry (Östlin et al. 2001). This mass discrepancy can be resolved if it is assumed that the width of the Hα line traces virial motions (see Melnick et al. 1987), indicating that these systems may be supported by velocity dispersion, i.e. random motions. This is rather unexpected for such gas-rich galaxies, but in line with the merger interpretation. Moreover, a few galaxies show peculiar rotation curves that initially rise rapidly, followed by a Keplerian (or even faster) decline, strengthening the interpretation that these galaxies are not in dynamical equilibrium (Östlin et al. 2001).

It is, however, well known that the ISM may be subject to other types of motions than purely gravitational. Winds and outflows, for example, are expected to be present in actively star forming galaxies like these. Possibly, the Hα velocity field traces feedback rather than the gravitational potential. Even if gravitational motions are likely to dominate bulk motions on the scale of a whole galaxy, this possibility underlines the need for information on the kinematical properties of the *stellar* component.

The near-IR [CaII]$_{\lambda\lambda 8498,8542,8662}$ triplet (hereafter Ca triplet) is well-suited for dynamical studies in galaxies

Send offprint requests to: G. Östlin,
e-mail: ostlin@astro.su.se

⋆ Based on observations collected at the European Southern Observatory, Paranal, Chile, under observing programme 71.B-0602.

dominated by young stellar populations (Dressler 1984). Even in a pure starburst, red supergiants will in most places contribute to an observable Ca triplet strength, and its use in probing complex galaxy kinematics has been demonstrated in many papers (e.g. Prada et al. 1996; Garcia-Lorenzo et al. 1997; Kormendy & Bender 1999; Márquez et al. 2003). We have therefore initiated a programme aimed at studying the stellar kinematics of BCGs, in particular those with peculiar Hα kinematics, by using the Ca triplet. Here, we are interested in studying the stellar kinematics as a function of radius, meaning that levels fainter than the night sky background need to be reached. This is a challenging task due to the many sky lines and strong fringing of most CCDs in this wavelength region. However, the red-optimised FORS2 spectrograph at the ESO VLT is ideally suited for this work.

Kobulnicky & Gebhardt (1997) studied the integrated dynamics of late type galaxies, among them a few BCGs, by looking at the [OII]$_{\lambda 3727}$ and CaII H and K lines. They found that stars and gas tend to have similar global profiles, but their results for low mass galaxies were inconclusive. Moreover, no LBCG was included in their study. The Ca H and K lines are not useful in our case due to strong emission lines in the blue spectral region.

Galaxies with masses and properties similar to local LBCGs are common at higher redshift and make a significant contribution to the cosmic star formation rate (e.g. Guzmán et al. 1997, 1997). Hence, local LBCGs may give insights into the early evolution of galaxies, and have luminosities high enough to be observable even at high redshift. However, the study of absorption lines relies on a strong continuum, and at high redshifts it will be challenging to observe anything but emission lines. As these are sensitive to dynamical feedback from star formation, it is an important task to investigate how well-coupled gaseous and stellar kinematics are in local galaxies of the same kind.

In this letter we report on the first results of our study: the first determination of the stellar kinematics of a BCG through the Ca triplet. In future papers we shall make a more detailed analysis and present the results for other galaxies in our sample.

1.1. ESO 400-G43

ESO 400-G43 is a luminous ($M_B = -19.6$, $H_0 = 75$ km s^{-1} Mpc^{-1}) BCG. It was once proposed as a young galaxy candidate (Bergvall & Jörsäter 1988), but deep surface photometry has revealed a rather massive underlying population (Bergvall & Östlin 2002). It has a companion galaxy at a projected distance of 70 kpc, too far for tidal forces to explain the strong starburst seen in ESO 400-G43 (Östlin et al. 2001).

The Hα velocity field is (upper right inset in Fig. 1), at first sight rather regular, but after an initial rise to 60 km s^{-1} at a radius of 1 kpc, the rotation curve falls off rapidly, in contrast to the photometric mass profile (Östlin et al. 2001). The fall is in fact faster than the Keplerian case, suggesting dynamical disequilibrium. The apparent rotational energy falls short of the photometric stellar mass by an order of magnitude. At much larger radii, ~15 kpc, the HI velocity is again close to the central 60 km s^{-1} (Bergvall & Jörsäter 1988) suggesting that a dynamical instability is responsible for the rapid decline of the optical rotation curve.

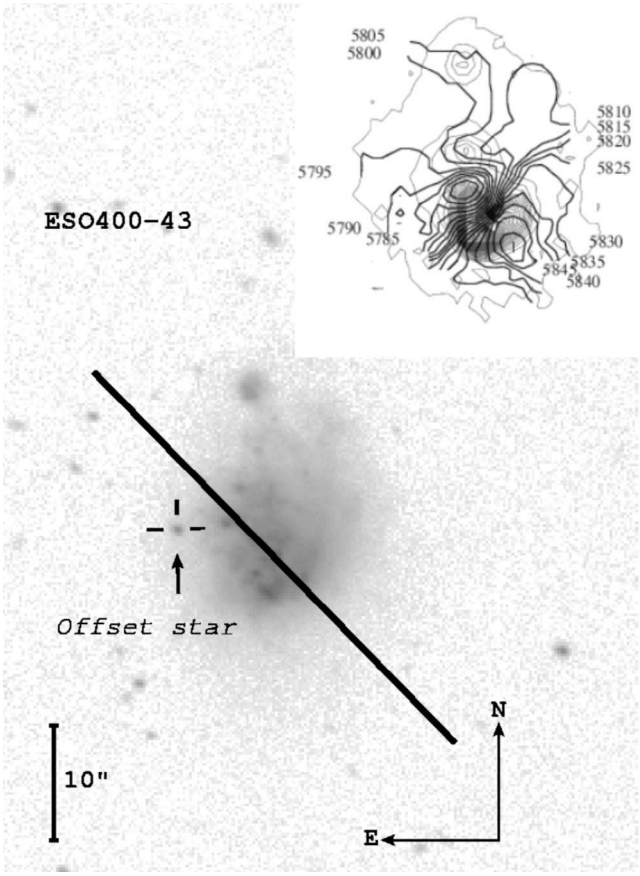

Fig. 1. FORS2 *I*-band image of ESO 400-G43 with the slit position indicated. The inset in the upper right corner shows the Hα velocity field from Östlin et al. (1999).

We identify three possible explanations for the apparent discrepancy between dynamical and photometrical mass. Gas–star decoupling may be important, i.e. a stellar velocity field different from the gaseous one, arising perhaps from outflows triggered by supernova winds or infall in a merging process. Alternatively, global gravitational instabilities might mean that neither stellar nor gaseous motions trace the potential. Finally, the low rotational velocities (but not the shape of the rotation curve) could be explained if velocity dispersion dominates the gravitational support.

The Hα velocity field has a well-defined kinematical centre and position angle, and was therefore suitable for a study with a single slit position. Our objective was to derive the stellar rotation curve and velocity dispersion out to a radius >2 kpc, making it necessary to reach surface brightness levels of $\mu_I \geq 21$ mag/arcsec^2.

2. Observations and reductions

The observations of ESO 400-G43 were obtained between June and August 2003 using the spectrograph FORS2 at the VLT. We observed one single slit position with a position angle of 45° (see Fig. 1), chosen to coincide with the kinematical

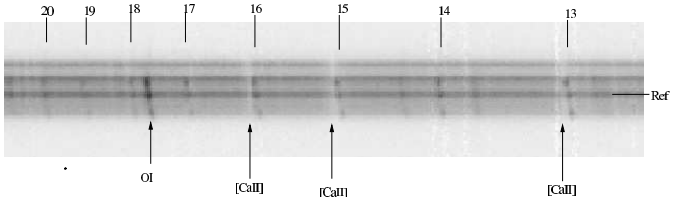

Fig. 2. Two-dimensional spectrum of ESO 400-G43. The Paschen emission lines have been marked and labelled with their number in the Paschen series above the spectrum. The CaII triplet lines and an OI emission line have been marked below the spectrum. On the right, the reference row is indicated. The height of the displayed part of the spectrum is 24″.

major axis derived from the Hα velocity field (see Fig. 1, and Östlin et al. 1999). We used the 1028z grism (covering λ = 773 to 948 nm) and a slit width of 0.7″, resulting in a spectral resolution of $R \sim 4000$ near the Ca triplet. The spectra were acquired as a series of 600 s exposures. In between each exposure, the telescope was offset along the slit. Using the same setup, six late-type reference stars were observed, to serve as templates for the cross correlation.

We used a somewhat non-standard reduction technique, in order to ensure effective subtraction of the strong atmospheric background emission at these wavelengths: adjacent pairs of exposures were subtracted from each other, each time scaling the subtracted frame so that residuals from the OH and O_2 lines were minimised. Only those frames resulting a in a good sky subtraction were retained for production of the final spectrum. Wavelength calibration was carried out in two dimensions using the OH sky lines on the unsubtracted frames. Each pairwise-subtracted frame was divided by a dome flatfield. The two-dimensional spectra were shifted to a common origin and coadded. Since the offset step along the slit was different in each case, negative residuals from objects incidentally falling in the slit cancelled when averaging the final frame. The resulting two dimensional spectrum (Fig. 2) was based on 14 frames with a total exposure time of 8400 s, which was used for the subsequent analysis. From this final two-dimensional spectrum, one-dimensional extractions were made, and flux-calibrated using spectra of the standard stars LTT 7379 and LTT 7987.

Our aim was to cross-correlate the extracted spectra with reference stars of different types, mainly late-type giants and supergiants. The galaxy spectra contain also narrow emission lines, most of which belong to the HI Paschen series. For each of the Ca triplet lines, there is a Paschen line (line number 13, 15 and 16 in the series) with only 3–4.5 Å higher rest wavelength. As the Ca absorption features have intrinsic widths of this order, the Paschen lines had to be removed before the Ca lines could be used to probe the stellar velocities.

To achieve this, we first measured the fluxes and velocities of the strongest unblended Paschen lines from our spectra, and compared with the predicted strengths for Case B recombination at a temperature of 10^4 K and density 100 cm^{-3} (Osterbrock 1989; Hummer & Storey 1987). Within the observational uncertainties, the lines follow the predicted values for zero reddening, consistent with the low extinction reported by

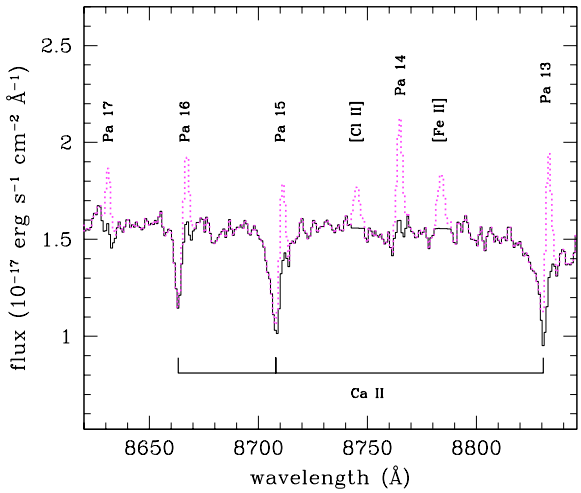

Fig. 3. An example of subtraction of Paschen lines. In this spectrum, the full drawn line shows the subtracted spectrum, which has also been interpolated across the emission lines of [Fe II] and [Cl II] The dotted line shows the unsubtracted spectrum.

Bergvall & Östlin (2002). We then modelled the Paschen series from Pa 9 to Pa 20 for each extracted spectrum, scaled to match the strongest clean Paschen lines and subtracted the modelled emission spectrum (Fig. 3). The redshifts and widths of the modelled lines were determined from the strongest Paschen lines in the spectrum.

Finally, we corrected for remaining strong emission lines like O I λ8446, [Cl II] λ8579 and [Fe II] λ8617, bad pixels and areas of poor sky subtraction by linearly interpolating across them. The spectra, now free of emission lines, were cross-correlated with the reference stars, using the IRAF task `fxcor` (see Tonry & Davis 1979). In addition to the Ca triplet, these spectra also contain other weak stellar absorption features which we also included in the cross correlation.

We calibrated the determination of $\sigma_\star$, the line of sight stellar velocity dispersion, by broadening the reference star spectra with Gaussians of various widths, then measuring the resulting FWHM of the cross-correlation peak.

3. Results and discussion

In Fig. 4 we show (filled squares) the stellar velocities and velocity dispersions along the slit, and the corresponding data for ionised gas from the Pa10 line (crosses) and [SIII]$_{\lambda 9069}$ (circles). The gas velocity dispersions have been corrected for the instrumental width. In addition the Hα velocities extracted from the Fabry-Perot interferometric data (Östlin et al. 1999) are shown (plus signs). For clarity, no error bars are plotted for the gas, but uncertainties are in general much smaller than for the stellar component.

The velocities for the ionised gas agree well with the previous investigations by Bergvall & Jörsäter (1988), and Östlin et al. (1999). The differences between the Pa lines and the Hα can be attributed to the poorer spatial resolution of the latter data. The velocities rise to ±55 km s^{-1} (uncorrected for inclination) over a linear scale of ±1.2 kpc. Outside these radii the velocities decline faster than the Keplerian case. On the

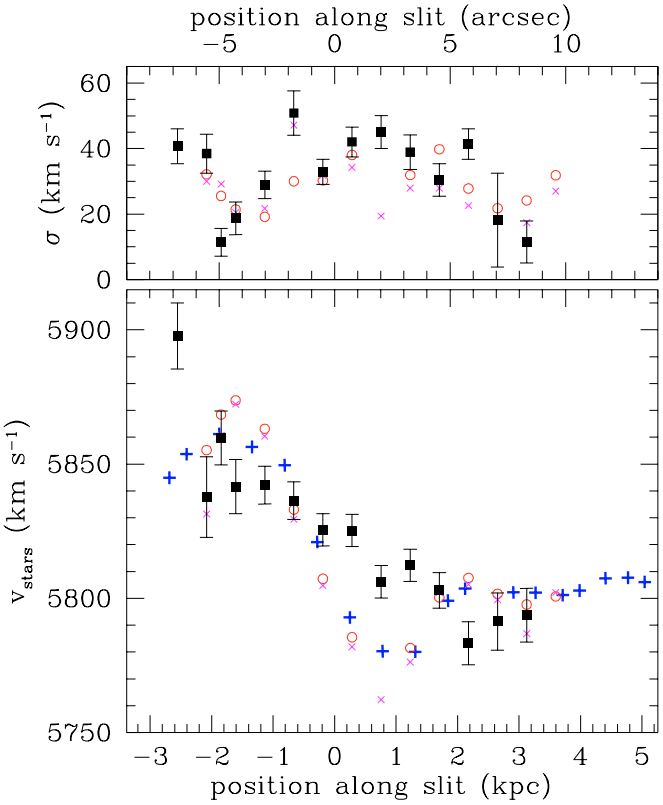

Fig. 4. Variation of heliocentric velocity (*bottom*) and velocity dispersion (*top*) in ESO 400-G43, measured from the absorption line spectrum. Squares with error bars represent stellar absorption data. Crosses (×) represent Pa10-lines, and circles [SIII] lines. Plus signs (+) show the Hα velocities for the same slit angle extracted from Fabry-Perot data (Östlin et al. 1999) using a sector opening angle of 5°. The scale in kpc (*bottom*) and arcsec (*top*) is indicated; the zero point coincides with the reference row in Fig. 2.

approaching side the gas velocities level out at radii ≥2 kpc. However, the difference with respect to the maximum velocity is still less than the Keplerian prediction. Hence, the ionised gas is not in dynamical equilibrium.

The stellar velocities behave differently. Firstly, the velocity gradient is much flatter than for the ionised gas. At $r = -2.2$ kpc there is a drop in the rotational velocity (Fig. 4), but at $r = -2.5$ kpc the rotation speed is again high. These two outer points are though the most uncertain ones, and there is no strong indication of a decline similar to what is seen in the gas. On the approaching side, the outer points suggest a modest velocity decrease at $r \geq 2.5$ kpc (Fig. 4), where a twist is seen in the Hα velocity field (see Fig. 1, and Östlin et al. 1999) as if a spiral arm were present. Taken together, the stellar velocity field is consistent with solid body rotation over the central ~12″ (5 kpc) of our spectrum, where the S/N is good.

The difference between the minimum and maximum stellar velocity is 124 km s^{-1}, but this is biased by the uncertain point at $r = -7''$. A straight line fit to the stellar velocities produces a velocity of ~80 km s^{-1} on a scale of 4.5 kpc (12″). With an assumed inclination of $i = 55°$ (Östlin et al. 1999) this implies a rotational amplitude of 50 km s^{-1}. Using the same simple formula as in Eq. (1) of Östlin et al. (1999, see also Lequeux 1983) with $f = 0.8$ gives a mass of $1.3 \times 10^9\ M_\odot$, somewhat lower than the photometric mass inside this radius of $3^{+3}_{-1} \times 10^9\ M_\odot$. The photometric mass profile indicates that the rotation curve should continue to rise out to a radius of 4 kpc (see Fig. 5 in Östlin et al. 2001). At $r = 2$ kpc the predicted circular speed for rotational support is 80^{+30}_{-15} km s^{-1}, whereas we measure $40/\sin(i)$ km s^{-1}.

This rotational measure assumes that the kinematical position angle for the stars coincides with that for the gas (45°). However, the major-axis position angle from the broad band isophotes and HI data is closer to 20°. Moreover, the broad-band data suggest a smaller inclination than 55°, while the HI kinematics imply $i \approx 50°$ (Bergvall & Jörsäter 1988). Hα/Hβ mapping (Östlin & Bergvall 1994) show that the south-eastern side of the disk is least affected by extinction and thus is probably nearest to us. With this orientation of the disk, an *outflow* would have the effect, which we also observe, that the kinematical position angle of the gas would be rotated anti-clockwise with respect to the stellar component. Consequently the mass from the stellar rotation curve may be underestimated, and should be increased by a factor of 1.9 (for $i = 55°$), or 2.3 if the true inclination is as low as 40°. In both cases, the mass inferred from the stellar rotation would be in fair agreement with the photometric mass.

The velocity dispersion measured from the ionised gas agrees well with that derived for the stars. Both are however lower than the 49 km s^{-1} derived from Fabry-Perot interferometry (Östlin et al. 2001). The widths we present in Fig. 4 are, however, close to the instrumental width and may be underestimated. The agreement between stars and gas suggests that the widths of the hydrogen recombination lines reflect motions in response to the gravitational potential (see Melnick et al. 1987). Under this assumption, Östlin et al. (2001) derived a mass of $8 \times 10^9\ M_\odot$. Taking $\sigma_\star \approx 40$ km s^{-1} we estimate the mass supported by stellar velocity dispersion to be $5 \times 10^9\ M_\odot$.

It is clear that the gaseous velocity field does not reflect dynamical equilibrium. A model that can reproduce the main features in both the stellar rotation curve and the Hα velocity field reasonably well is one with solid body rotation with a position angle of 20° and an outflow with a 30 km s^{-1} expansion velocity out to a radius of ~3 kpc, where the expansion is halted in a shock. However, this model is not well constrained. A two-dimensional stellar velocity field would be required in order to construct a physical model for the kinematics and distinguish between the possible explanations given in Sect. 1.1.

4. Conclusions

The gaseous rotation curve of ESO 400-G43 increases steeply within 1 kpc from the kinematical centre, then drops faster than the Keplerian prediction. This is not seen in the stellar rotation curve which presents a solid body shape out to $r = 2$ kpc. Hence, stars and gas are dynamically decoupled in this galaxy. The reasons for this could be outflows due to feedback from star formation or dynamical instabilities in a merging process, and will be discussed in future papers.

The stellar and gaseous velocity dispersions agree, but the amount of stellar velocity dispersion is somewhat smaller than

implied by the photometric mass of $12^{+16}_{-4} \times 10^9\ M_\odot$ (Östlin et al. 2001). Nevertheless, even allowing for uncertainties in the inclination, the stellar velocity dispersion makes a larger contribution than rotation to the gravitational support. This is consistent with the picture that the starburst host galaxy could be of, or will evolve into, elliptical type (see Bergvall & Östlin 2002).

Even though the stellar and gaseous kinematics appear decoupled in this galaxy, the mass inferred from the line widths of nebular lines and stellar absorption features agree. It remains to be seen if this is a general feature of luminous BCGs, but if so, it would lend credibility to mass estimates of high redshift galaxies that are based on the widths of narrow nebular lines.

Acknowledgements. We thank our colleagues R. Guzmán and T. Marquart for stimulating discussions and useful suggestions. This work was supported by the Swedish Research Council.

References

Amram, P., Boulesteix, J., Georgelin, Y. P., et al. 1991, Msgr, 64, 44
Bergvall, N., & Jörsäter, S. 1988, Nature, 331, 589
Bergvall, N., & Östlin, G. 2002, A&A, 390, 891
Dressler, A. 1984, ApJ, 286, 97
Garcia-Lorenzo, B., Mediavilla, E., Arribas, S., & del Burgo, C. 1997, ApJ, 483, L99
Guzmán, R., Gallego, J., Koo, D. C., et al. 1997, ApJ, 489, 559
Guzmán, R., Östlin, G., Kunth, D., et al. 2003, ApJ, 586, L45
Hummer, D. G., & Storey, P. J. 1987, MNRAS, 224, 801
Izotov, Y. I., & Thuan, T. X. 1999, ApJ, 511, 639
Kobulnicky, H., & Gebhardt, K. 2000, AJ, 119, 1608
Kormendy, J., & Bender, R. 1999, ApJ, 522, 772
Kunth, D., & Östlin, G. 2000, A&ARv, 10, 1
Lequeux, J. 1983, A&A, 125, 394
Márquez, I., Masegosa, J., Durret, F., et al. 2003, A&A, 409, 459
Melnick, J., Moles, M., Terlevich, R., & Garcia-Pelayo, J. M. 1987, MNRAS, 226, 849
Osterbrock, D. 1989, Astrophysics of gaseous nebulae and active galactic nuclei (Mill Valley: University Science Books)
Östlin, G., & Bergvall, N. 1994, in ESO/OHP workshop on dwarf galaxies, ed. G. Meylan, & P. Prugniel, ESO Conf. Workshop Proc., 49, 451
Östlin, G., Amram, P., Masegosa, J., Bergvall, N., & Boulesteix, J. 1999, A&AS, 137, 419
Östlin, G., Amram, P., Bergvall, N., et al. 2001, A&A, 374, 800
Papaderos, P., Loose, H.-H., Fricke, K. J., & Thuan, T. X. 1996, A&A, 314, 59
Prada, F., Gutierrez, C. M., Peletier, R. F., & McKeith, C. D. 1996, ApJ, 463, L9
Searle, L., & Sargent, W. 1972, ApJ, 173, 25
Tonry, J., & Davis, M. 1979, AJ, 84, 1511
van Zee, L., Skillman, E. D., & Salzer, J. J. 1998, AJ, 116, 1186